The Pathology of the Feline Model of Mucopolysaccharidosis VI

Mark E. Haskins, VMD, PhD, Gustavo D. Aguirre, VMD, Peter F. Jezyk, PhD, VMD, Donald F. Patterson, DVM, DSc

Three cats with feline arylsulfatase-B-deficient mucopolysaccharidosis were studied by light and transmission electron microscopy. Membrane-bound cytoplasmic inclusions were present in hepatocytes, bone marrow granulocytes, vascular smooth muscle cells, and fibroblasts in skin, cornea, and cardiac valves. Central nervous system lesions were restricted to mild ventricular dilatation, perithelial cell vacuolation, and, in one animal, cord compression by vertebral exostoses. The lesions in these cats closely resembled those described in human patients with mucopolysaccharidosis VI (Maroteaux-Lamy syndrome). (Am J Pathol 1980, 101:657-674)

THE GENETIC MUCOPOLYSACCHARIDOSES (MPS) are a group of diseases which result from defects in glycosaminoglycan (GAG) metabolism. At present, there are 10 subclassifications in man, each of which has a characteristic combination of clinical signs, urinary GAG excretion, and a specific lysosomal enzyme deficiency.[1-3]

Two of these subclasses have recently been described in domestic cats.[4-9] This report describes the clinical features and the gross, histologic, and ultrastructural pathologic features of MPS VI (Maroteaux-Lamy syndrome) in cats and compares the lesions in cats with those described in man.

Materials and Methods

Three cats clinically affected with mucopolysaccharidosis were utilized in this study. The animals excreted excess dermatan sulfate in the urine. Activity of the enzyme arylsulfatase B in peripheral leukocytes was markedly decreased (8.2, 10.4, and 13.2 vs 129 nmoles *p*-nitrocatechol sulfate hydrolyzed/hr/mg protein in leukocytes from normal animals).[8] Two of the animals were Siamese, 2- and 5-year-old females (Cats 1 and 3, respectively, Text-figure 1) that were raised as house pets until donated by the owners. The third, a 10-month-old black male (Cat 2), was produced within the Medical Genetics animal colony of the School of Veterinary Medicine, University of Pennsylvania, by breeding an obligate carrier male (Siamese) to one of his carrier daughters (Siamese–domestic short-haired cross).

One clinically normal Siamese cat, having leukocyte arylsulfatase B levels within normal limits, was used as a control animal for electron-microscopic studies.

From the Sections of Pathology, Ophthalmology, and Medical Genetics, School of Veterinary Medicine, University of Pennsylvania, University of Pennsylvania Genetics Center, and the Department of Ophthalmology, School of Medicine and Scheie Eye Institute, University of Pennsylvania, Philadelphia, Pennsylvania.

Supported by NIH Genetics Center Grant GM-20138 and NIH Grants AM-25759 and EY-3400.

Address reprint requests to Dr. Mark Haskins, Sections of Pathology and Medical Genetics, University of Pennsylvania, School of Veterinary Medicine, 3800 Spruce Street, Philadelphia, Pennsylvania 19104.

0002-9440/80/1209-0657$01.00

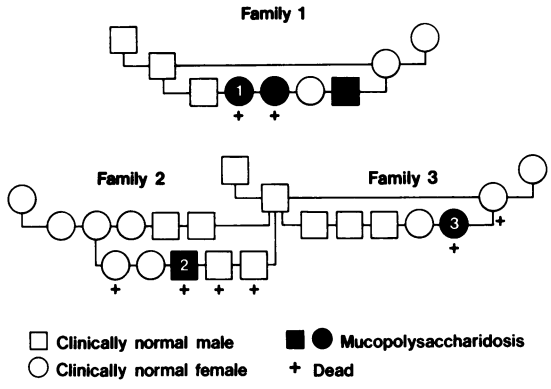

TEXT-FIGURE 1—The pedigree of 3 families of inbred cats with mucopolysaccharidosis VI. The individuals described in this report are a 2-year-old female (Cat 1), a 10-month-old male (Cat 2), and a 5-year-old female (Cat 3).

The animals were killed by intravenous administration of an overdose of barbiturate and necropsied. Unfixed tissue samples were frozen in liquid nitrogen and processed by one of two methods: 1) tissues were sectioned on an IEC CTF microtome-cryostat and stained with periodic acid–Schiff and alcian blue; 2) tissues were freeze-dried, embedded in paraffin, dry-sectioned, and placed on an albumin-coated glass slide, heated (45 C) overnight, treated with CTAB, stained with 1% alcian blue in 1% glacial acetic acid (pH 2.7) and counterstained with nuclear red. Tissue samples for routine light-microscopic examination were fixed in 10% buffered formalin, paraffin-embedded, sectioned, and stained with hematoxylin and eosin. Bone for light-microscopic examination was immersed in 15% formic acid for 1 week and then, under negative pressure, treated progressively with water, alcohol, xylene, and paraffin. Ten-micron sections were stained with hematoxylin and eosin. Tissue samples for ultrastructural examination were fixed overnight in cacodylate-buffered glutaraldehyde at 4 C, postfixed in osmium tetroxide, dehydrated, and embedded in Spurr's medium [10] or Epon.[11] One-micron-thick sections were stained with azure II–methylene blue for light-microscopic examination. Ultrathin sections (silver interference) were taken from selected areas, stained with uranyl acetate–lead citrate, and examined with a Zeiss EM 9S-2 transmission electron microscope.

Results

Clinical History

All 3 affected cats had facial dysmorphia, with a small head, broad shortened maxilla, and small ears. Each had diffuse bilateral corneal clouding resulting from fine granular opacities present at all levels of the corneal stroma when observed with a slit lamp biomicroscope. The facial dysmorphia and corneal clouding were first observed at 8 weeks of age in the animal raised in our colony. Radiographic osseous change was most severe in the oldest cat, but all 3 animals showed evidence of epiphyseal dysplasia of the long bones and cervical spine, bilateral hip subluxation, pectus excavatum, and odontoid hypoplasia.[8] There was a variable degree of generalized osteoporosis present radiographically as well as an increased opacity (sclerosis) at the vertebral endplates and articular facets.

The youngest animal (Cat 2, Text-figure 1) had evidence of ventral spondylosis in the thoracic spine. The skeletal lesions, observed for 2 years in the oldest animal (Cat 3), were progressive.

The oldest animal also had progressive locomotor difficulty, the severity of which reflected the degree of skeletal disease. At 7 months of age Cat 2 developed hind limb paresis with depressed pain perception and increased extensor tone. The animal retained some voluntary control of hind limb movement and was not incontinent. Vertebral subluxation at T_{13}-L_1 was diagnosed radiographically. Other than the above, the animals appeared neurologically intact, active, alert, and responsive.

At 18 months of age Cat 1 developed cutaneous nodules, 4–10 mm in diameter, over her face and head. These nodules were not pruritic, gradually regressed, and were not apparent 6 weeks later. Bacterial and fungal cultures of biopsied tissue were negative.

Necropsy Findings

Liver

Grossly the livers were of normal size and texture. By light microscopy hepatocellular vacuolation was not apparent; however, Kupffer cells and interlobular connective tissue cells contained clear areas, some multiloculated, within the cytoplasm. Seen by electron microscopy, hepatocytes contained up to 20 small (0.5–1.5 μ in diameter), membrane-bound granular inclusions (Figure 1). Interlobular connective tissue cells and Kupffer cells were swollen with membrane-bound inclusions, which were either empty or contained granular material (Figure 2).

Spleen

Grossly the spleens appeared normal. Seen by light microscopy, the smooth muscle cells of the trabeculae contained cytoplasmic vacuoles that did not distort the cell shape. These vacuoles were electron-lucent and membrane-bound and contained remnants of myelin-like figures (Figure 3).

Eye

Intracytoplasmic vacuoles were present in the cytoplasm of fibroblasts in the cornea (Figure 4), conjunctiva, iris, sclera, choroid, intrascleral and choroidal nerves, extraocular muscles, and optic nerve. The cytoplasmic volume was increased and cell contours were altered (hypertrophy) by the accumulation of variably sized vacuolated inclusions. By electron microscopy, most of the vacuoles appeared electron-lucent, although a faint

granular matrix of lamellar membranous pattern remained in some (Figure 5).

In tissue of neuroectodermal origin, the presence of vacuolated intracytoplasmic inclusions varied with the degree of melanin pigmentation. The pigmented iridal and ciliary epithelial cells were normal. The nonpigmented ciliary epithelium, analogous to the inner layer of the embryonic optic cup, was hypertrophied (Figure 6). The cytoplasm contained many vacuolated inclusions, which displaced the nuclei apically and compressed the adjacent and otherwise normal pigmented ciliary epithelium.

The variation in ocular disease between pigmented and nonpigmented regions was best illustrated in the retinal pigment epithelium. (In the cat the retinal pigment epithelium overlying the tapetum lucidum is *not* pigmented [tapetal pigment epithelium]; the epithelium in areas without a tapetum is pigmented [nontapetal pigment epithelium].[12]) The tapetal pigment epithelium contained many intracytoplasmic vacuolated inclusions (Figure 7). Some cells were markedly hypertrophied, resulting in shortening and disorientation of adjacent photoreceptor outer segments. On the other hand, the nontapetal pigment epithelium of the periphery contained no vacuolated inclusion as seen by either light or electron microscopy. In some areas of the posterior pole, especially in the 10-month-old black cat, nontapetal pigment epithelial cells contained small to large aggregates of vacuolated inclusions. In these areas, however, the pigment epithelial abnormalities were not as uniform and extreme as observed in the nonpigmented tapetal pigment epithelium. Ultrastructural examination of the affected pigment epithelial cells indicated that the electron-lucent inclusions were membrane-bound; some contained a fine granular to lamellar matrix.

Skeleton

As seen by light microscopy, the articular cartilage of the stifle (knee) of the oldest animal was hypercellular. Large bundles of normal-appearing collagen were covered by synovium; the subchondral plate appeared sclerotic and contained islands of cartilage. The medullary cavity of the metaphysis was bone-free, lacking endosteal spicules. Tide lines of ossified cartilage were present in some areas; however, the epiphyseal trabeculae were thicker than normal. The cervical vertebrae were deformed and contained islands of cartilage, fibrocartilage, and fibrous tissue. Bony bridges between vertebrae were present both dorsally and ventrally (Figure 8). No normal intervertebral disks could be identified. Cartilage in all 3 animals, from both the rib and the articular surface of the proximal tibia, contained large cells with a trabecular cytoplasm. Seen by electron mi-

croscopy, these cells were packed with membrane-bound, empty inclusions (Figure 3).

Central Nervous System

The lateral cerebral ventricles of the brains of all 3 cats were larger than normal, all to an approximately equal degree. Histologically, large cells containing vacuolated cytoplasm were present in the connective tissue of the meninges and choroid plexi.

The spinal cord from the 10-month-old cat with radiographic evidence of vertebral subluxation (T_{13}-L_1) contained dorsolateral depressions immediately caudal to the nerve roots at T_{13}, L_1, and L_2 (Figure 10). The cord was gray–brown in this area. The histologic appearance of the cord in the depressed areas was abnormal in its outline. The peripheral white matter contained multiple foci of vacuolation with some debris present but no evidence of myelophagia, astrocytosis, or increased vascularity. One swollen axon was noted. The nerve roots fit into indentations along the cord, indicating compression. The duramater was of normal thickness.

The only electron-microscopic abnormality noted was the presence of membrane-bound inclusions in the cytoplasm of perivascular cells of the brain and cord.

Other Systems

Skin: Fibroblasts in skin taken at postmortem examination did not appear abnormal by light microscopy. However, by electron microscopy membrane-bound myelin-like figures were present in the cytoplasm of dermal fibroblasts (Figure 11). The nodules present on the face and head of Cat 1 were biopsied several months prior to death. Present in the dermis were large macrophagelike cells which contained vesicular cytoplasm. There was no evidence of an inflammatory cell response or any substance present between cells or collagen bundles.

Cardiovascular: Grossly, the left atrioventricular valves appeared thickened, white, and nodular. Seen by light microscopy, fibroblasts in the valves and cordae tendinae appeared ballooned, with a finely vesicular cytoplasm (Figure 12), which was packed with membrane-bound vesicles when examined electron-microscopically (Figure 13).

Seen by light microscopy, swollen smooth muscle cells were present in the media of the aorta and coronary arteries (Figure 14).

Bone Marrow: The inclusions present in cells of the granulocytic series contained granular (Figure 15), lamellar, and/or crystalloid figures similar to those previously described in peripheral blood polymorphonuclear (PMN) leukocytes.[7,8]

Discussion

The clinical syndrome of MPS VI in the feline parallels quite closely the syndrome in man. Both have facial dysmorphia, corneal clouding, osseous change characterized by epiphyseal dysplasia, peripheral leukocyte granulation, urinary excretion of excessive amounts of dermatan sulfate, and a deficiency of arylsulfatase B.[6-9] Neurologic complications in man may include carpal tunnel syndrome, myelopathy secondary to C_1-C_2 subluxation [13] and/or cervical cord compression associated with thickening of the cervical dura.[14] In the cat posterior paresis was seen concomitant with bony encroachment upon the thoracolumbar spinal cord. Skin nodules similar to those seen in one of the cats have not been reported in MPS VI in man; however, small cutaneous papules and nodules have been reported to occur over the chest, back, and extremities in human patients with MPS II (Hunter's syndrome).[15-19]

The pathology of the feline disease also closely parallels that of the human mucopolysaccharidoses in general and MPS VI in particular. The basic lesion in these diseases involves the storage of GAGs within membrane-bound cytoplasmic inclusions (lysosomes), the consequences of which may include alteration of cell shape, size, and function. The accumulation of GAG is also thought to inhibit other lysosomal enzymes, which may lead to the accumulation of other products, particularly glycolipids.[20,21] This may explain the presence, seen ultrastructurally, of lamellar and/or myelinlike inclusions in a disease where only empty or granular inclusions would be expected.

Hepatosplenomegaly was not a prominent feature of the disease in the cat, but the presence of small granular inclusions in hepatocytes and Kupffer cells is similar to that described in the livers of human MPS VI patients.[22,23] A description of the ultrastructure of the spleen has not been reported in MPS VI in man.

With the exception of the retinal pigment epithelial abnormalities, the characteristic lesion and its distribution in ocular tissues appears to be quite similar in man and cat.[30,31] Unlike man, the retinal pigment epithelium (RPE) of the cat has pigmented and nonpigmented zones. In feline MPS VI, the nonpigmented epithelium contained marked accumulations of vacuolated inclusions, which resulted in hypertrophy of one or several pigment epithelial cells. The pigmented pigment epithelium, on the other hand, was normal or mildly affected. The differences in the disease between these two areas and the possible influences of pigmentation is under investigation at this time. Since the RPE of man is pigmented, a different manifestation of the disease, when compared with the cat, is to be expected.

The skeletal lesions described for the mucopolysaccharidoses in general [19,24] closely resemble those in the feline model; the alterations being in areas of enchondral calcification. These areas are characterized by the presence of irregular islands of unossified tissue, irregular zones of provisional calcification, and swollen cartilage cells containing large numbers of cytoplasmic membrane-bound inclusions, which are densely packed and frequently coalescent. Such alterations in enchondral calcification may result from an inability to shift GAG concentration. The precise role of GAG in calcification is not clear; however, shifts in GAG concentrations are associated with mineralization and are considered important in normal bone development and remodeling.[25,26]

Reports of central nervous system pathology in human cases of MPS VI have been limited to discussions of hydrocephalus.[13,27] It is not clear in cats that the enlarged lateral ventricles represent "true" hydrocephalus, because the dilatation was not marked, the condition did not appear to be progressive, and it was not associated with clinical signs. Descriptions of CNS lesions in human patients with MPS VI have not been reported. There is, however, a report of the histologic and histochemical appearance of the brain in MPS V (presently classified MPS IS), another one of the MPS diseases. Like MPS VI, MPS V is also characterized by normal intelligence.[28] The neurons in the patient with MPS V were normal. However, there were perithelial cell lesions similar to those reported in other MPS diseases in man [19,22,28,29] and similar to those seen in these cats.

Thickened tricuspid and mitral valves containing large cells with granular cytoplasm have been observed in human patients with MPS VI. These lesions clinically may result in hemodynamic abnormalities.[32] Valvular thickening is also present in other MPS syndromes but is prominent in MPS IS and VI because of the long survival of these patients.[19,32] The electron-microscopic appearance of fine reticulogranular inclusions in valvular cells is similar to that observed in these cats.[19,33] Other cardiovascular lesions of the MPS diseases in man include thickening of the cordae tendinae and their insertions, endocardial thickening, clear cells, intimal thickening, and atherosclerotic change of the aorta.[19,33–35] Of these, thickening of the cordae and vacuolated aortic smooth muscle cells were seen in the cats.

The pathology of the skin in MPS VI in man is similar to that seen in the cat, and it is characterized by subepidermal connective tissue cell vacuolation.[31] Ultrastructurally the fibroblasts contain membrane-bound cytoplasmic inclusions, often in coalescing clusters, which are electron-lucent or contain a fine granular matrix and membranous lamellar material.[31,36,37] The cutaneous nodules of MPS II discussed clinically above

have been reported to result from an extracellular collection of metachromatic material in the lower reticular dermis, producing a separation of collagen bundles.[18] The skin nodules observed in one cat did not have this appearance, the predominant lesion being the presence of large rounded vesicular cells. These cells could represent macrophages that have phagocytosed extracellular material.

Feline MPS VI, with its clinical, biochemical, and pathologic similarities to MPS VI in man, should prove to be a useful model in the study of lysosomal storage disease pathogenesis and approaches to therapy. This is particularly true because not only is the cat an excellent species for laboratory investigation, but animals with this disease survive comfortably for many years, thus allowing chronic therapeutic trials.

References

1. Dorfman A, Matalon R: The mucopolysaccharidoses: A review. Proc Natl Acad Sci USA 1976, 73:630–637
2. McKusick VA, Neufeld EF, Kelly TE: The mucopolysaccharide storage diseases, The Metabolic Basis of Inherited Disease. 4th edition. Edited by JB Stanbury, JB Wyngaarden, DS Fredrickson. New York, McGraw Hill, 1978, pp 1282–1307
3. Neufeld EF, Lim TW, Shapiro LJ: Inherited disorders of lysosomal metabolism. Annu Rev Biochem 1975, 44:357–376
4. Haskins ME, Jezyk PF, Desnick RJ, McDonough SK, Patterson DF: Mucopolysaccharidosis in a domestic short-haired cat: A disease distinct from that seen in the Siamese cat. J Am Vet Med Assoc 1979, 175:384–387
5. Haskins ME, Jezyk PF, Desnick RJ, McDonough SK, Patterson DF: Alpha-L-iduronidase deficiency in a cat: A model of mucopolysaccharidosis I. Ped Res 1979, 13:1294–1297
6. Cowell KR, Jezyk PF, Haskins ME, Patterson DF: Mucopolysaccharidosis in a cat. J Am Vet Med Assoc 1976, 169:334–339
7. Jezyk PF, Haskins ME, Patterson DF, Mellman WJ, Greenstein M: Mucopolysaccharidosis in a cat with arylsulfatase B deficiency: A model of Maroteaux-Lamy syndrome. Science 1977, 198:834–836
8. Haskins ME, Jezyk PF, Patterson DF: Mucopolysaccharide storage disease in three families of cats with arylsulfatase B deficiency: Leukocyte studies and carrier identification. Ped Res 1979, 13:1203–1210
9. Haskins ME, Jezyk PF, Desnick RJ, Patterson DF: Feline models of mucopolysaccharidosis, Enzyme Therapy in Genetic Disease. Vol 2. Edited by RJ Desnick. New York, AR Liss, 1980, pp 219–224
10. Spurr AR: A low-viscosity epoxy resin embedding medium for electron microscopy. J Ultrastruct Res 1969, 26:31–43
11. Luft JH: Improvements in epoxy resin embedding methods. J Biophys Biochem Cytol 1961, 9:409–414
12. Aguirre GD, Rubin LF: Diseases of the retinal pigment epithelium in animals, The Retinal Pigment Epithelium. Edited by K Zinn, M Marmor. Cambridge, Harvard University Press, 1979, pp 334–356
13. McKusick V: The mucopolysaccharidoses, Heritable Disorders of Connective Tissue. St. Louis, C. V. Mosby, 1972, pp 521–686

14. Peterson DI, Bacchus H, Seaich L, Kelly TE: Myelopathy associated with Maroteaux-Lamy syndrome. Arch Neurol 1975, 32:127–129
15. Hunter C: A rare disease in two brothers. Proc R Soc Med 1917, 10:104–116
16. Prystowsky SD, Maumenee IH, Freeman RG, Herndon JH, Harrod MJ: A cutaneous marker in the Hunter syndrome. Arch Dermatol 1977, 113:602–605
17. Kelly TE: The mucopolysaccharidoses and mucolipidoses. Clin Ortho Related Res 1976, 114:116–136
18. Freeman RG: A pathological basis for the cutaneous papules of mucopolysaccharidosis II (the Hunter syndrome). J Cutan Pathol 1977, 4:318–328
19. Spranger J: The systemic mucopolysaccharidoses. Ergebnisse der Luneren Midizin und Kinderheilkunde. Edited by P Frick, B-A von Harnack, AF Muller, A Prader, R Schonen, R Wolff. New York, Springer-Verlag, 1972, pp 165–265
20. Avila JL, Convit J: Inhibition of leucocytic lysosomal enzymes by glycosaminoglycans *in vitro*. Biochem J 1975, 152:57–64
21. Kint JA, Dacremont G, Carton D, Orye E, Hooft C: Mucopolysacccharidosis: Secondarily induced abnormal distribution of lysosomal isoenzymes. Science 1973, 181:352–354
22. Tondeur M, Neufeld EF: The mucopolysaccharidoses—Biochemistry and ultrastructure, Molecular Pathology. Edited by RA Good, SB Day, JJ Yunis. Springfield, Ill, Charles C Thomas, 1975, pp 600–621
23. Van Hoof F, Hers HG: The mucopolysaccharidoses as lysosmal diseases, Sphingolipids, Sphingolipidoses and Allied Disorders. Edited by BW Volk, SM Aronson. New York, Plenum Press, 1972, pp 211–223
24. Silberberg R, Rimoin DL, Rosenthal RE, Hasler MB: Ultrastructure of cartilage in the Hurler and Sanfilippo syndromes. Arch Pathol 1972, 94:500–510
25. de Bernard B, Stagni N, Colautti I, Vittur F, Bonucci E: Glycosaminoglycans and endochondral calcification. Clin Orthop 1977, 126:285–291
26. Rasmussen H, Bordier P: Physiological and cellular basis of metabolic bone disease. Baltimore, Williams & Wilkins, 1974, pp 88–90
27. Goldberg MF, Scott CI, McKusick VA: Hydrocephalus and papilledema in the Maroteaux-Lamy syndrome (Mucopolysaccharidosis type VI). Am J Opthalmol 1970, 69:969–975
28. Dekaban AS, Constantopoulos G: Mucopolysaccharidosis types I, II, IIIA and V: Pathological and biochemical abnormalities in the neural and mesenchymal elements of the brain. Acta Neuropathol (Berl) 1977, 39:1–7
29. Loeb H, Jonniaux G, Resibois A, Cremer N, Dodion J, Tondeur M, Gregoire PE, Richard J, Cieters P: Biochemical and ultrastructural studies in Hurler's syndrome. J Pediatr 1968, 73:860–874
30. Kenyon KR, Topping TM, Green WR, Maumenee AE: Ocular pathology of the Maroteaux-Lamy Syndrome (Systemic mucopolysaccharidosis type VI): Histologic and ultrastructural report of two cases. Am J Ophthalmol 1972, 73:718–741
31. Quigley HA, Kenyon KR: Ultrastructural and histochemical studies of a newly recognized form of systemic mucopolysaccharidosis (Maroteaux-Lamy syndrome, mild phenotype). Am J Ophthalmol 1974, 77:809–818
32. Spranger JW, Koch F, McKusick VA, Natzschka J, Wiedmann HR, Zellweger H: Mucopolysaccharidosis VI (Maroteaux-Lamy's disease). Helv Paediatr Acta 1970, 25:337–362
33. Lagunoff D, Ross R, Benditt EP: Histochemical and electron microscopic study in a case of Hurler's disease. Am J Pathol 1962, 41:273–286
34. Glober GA, Tanaka KR, Turner JA, Liu CK: Mucopolysaccharidosis, an unusual cause of cardiac valvular disease. Am J Cardiol 1968, 22:133–136
35. Okada R, Rosenthal IM, Scaravelli G, Lev M: A histopathologic study of the heart in gargolism. Arch Pathol 1967, 84:20–30

36. Pilz H, von Figura K, Goebel HH: Deficiency of aryl-sulfatase B in 2 brothers aged 40 and 38 years (Maroteaux-Lamy Syndrome, type B). Ann Neurol 1979, 6:315–325
37. Kenyon DR, Quigley HA, Hussels IE, Wyllie RG: The systemic mucopolysaccharidoses: Ultrastructure and histochemical studies of conjunctiva and skin. Am J Ophthalmol 1972, 73:811–833

Acknowledgments

The authors thank Drs. J. T. McGrath, W. H. Riser, and A. W. Fetter for their invaluable assistance in interpretation and B. Montabana, M. Connelly, and D. Ringler for their excellent technical assistance.

Figure 1—Electron micrograph of a hepatocyte which contains numerous membrane bound granular inclusions (*arrows*). (Uranyl acetate–lead citrate, ×1900)

Figure 2—Electron micrograph of a periportal connective tissue cell swollen with cytoplasmic vacuoles. *E* = bile duct epithelium. (Uranyl acetate–lead citrate, ×4800)

Figure 3—Electron micrograph of a smooth muscle cell from a splenic trabeculae. Most cytoplasmic vacuoles contain remnants of myelin-like figures (*arrows*). (Uranyl acetate–lead citrate, ×4800)

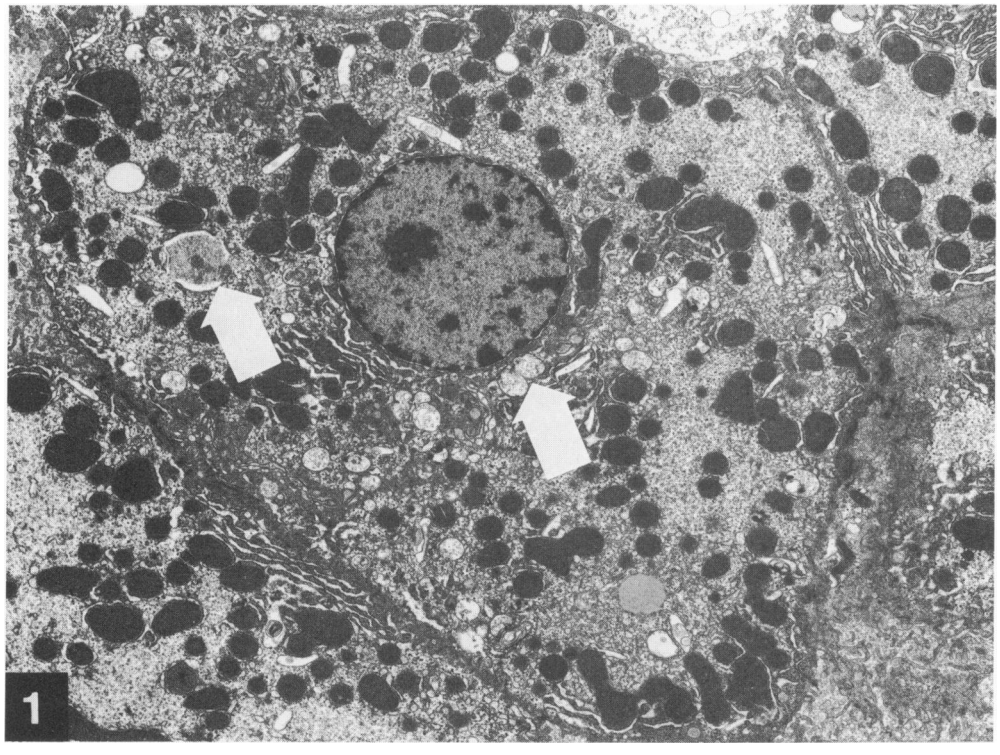
1

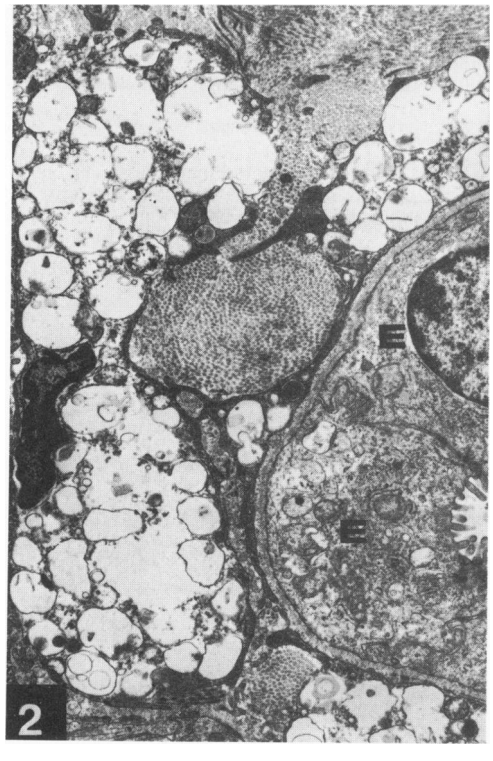
E
E
2

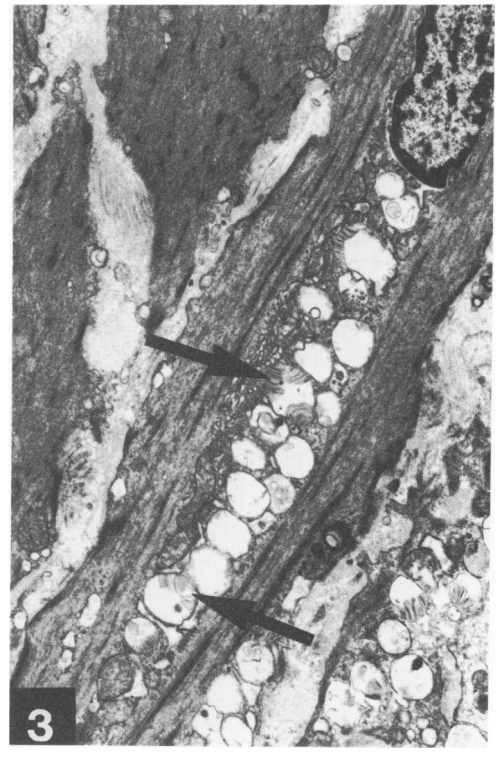
3

Figure 4—The keratocytes (*arrows*) in the posterior cornea are enlarged due to the intracellular accmulation of inclusions. Descemet's membrane (D) and endothelium (*arrowhead*) are normal. (Azure II–methylene blue, ×630)

Figure 5—The keratocytic cytoplasm contains numerous electron-lucent vacuoles, which are membrane-bound (*arrows*). The adjacent corneal stroma (*S*) is normal. (Azure II–methylene blue, ×16,600)

Figure 6—A longitudinal section of ciliary processes demonstrates swelling of the nonpigmented epithelium (*arrowheads*) secondary to the accumulation of vacuolated inclusion. The nuclei are displaced apically (*arrows*) and compress the adjacent pigmented ciliary epithelial cells. A fibroblast (*F*) in the stroma of the ciliary process also contains vacuolated inclusions. (Azure II–methylene blue, ×400)

Figure 7—Nonpigmented tapetal pigment epithelial cells contain vacuolated inclusions. The 3 cells on the right are massively hypertrophied, and thus photoreceptor outer segment shortening occurs. The choriocapillaris (*arrowheads*) indents the basal pigment epithelium. (Uranyl acetate–lead citrate, ×630)

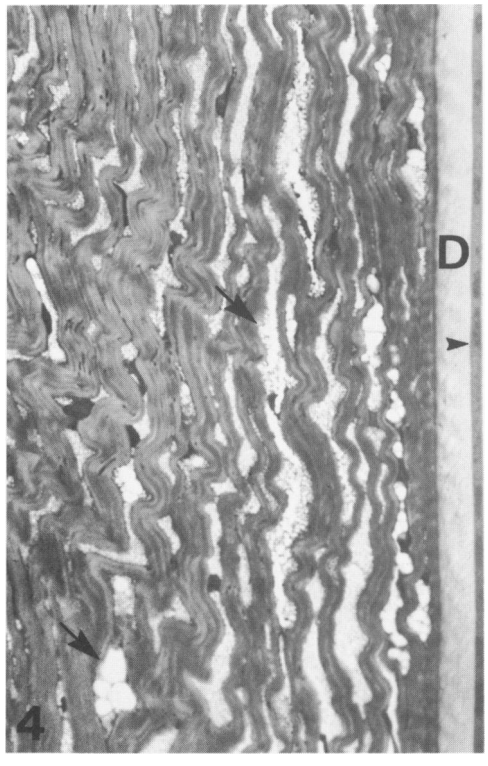
D
4

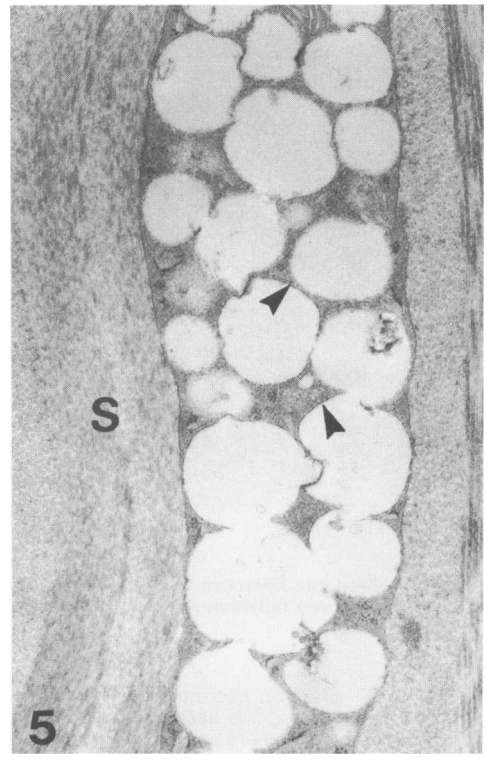
S
5

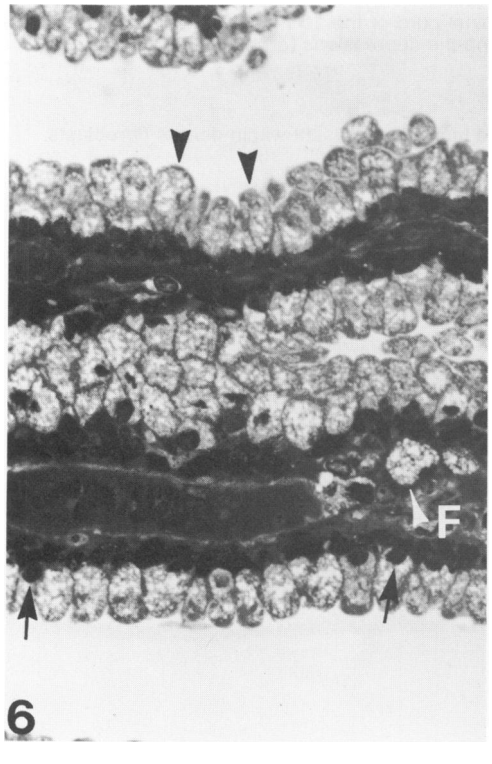
F
6

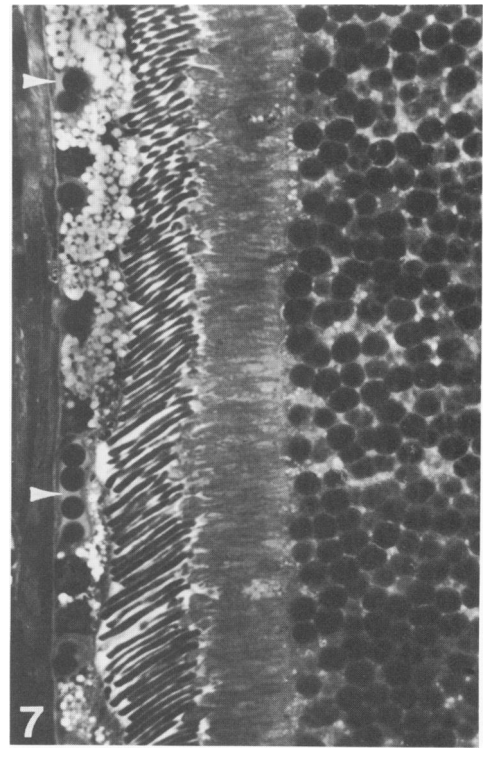
7

Figure 8—Light micrograph of the cervical spine of the 5-year-old female cat. Note the bony bridge (*arrows*) between the vertebral bodies. The intervertebral tissue is primarily cartilage. (H&E, ×10)

Figure 9—Electron micrograph of a cartilage cell from the articular surface of the proximal tibia. The cytoplasm is packed with membrane-bound empty inclusions, which appear to have coalesced in some areas (*arrow*). (Uranyl acetate–lead citrate, ×1900)

Figure 10—Photograph of the thoracolumbar spinal cord of the 10-month-old cat with posterior paresis. Note the discoloration of the cord and the depressions (*arrows*) just caudal to the nerve roots.

Figure 11—Electron micrograph of the myelinlike inclusions present within dermal fibroblasts. (Uranyl acetate–lead citrate, ×28,000)

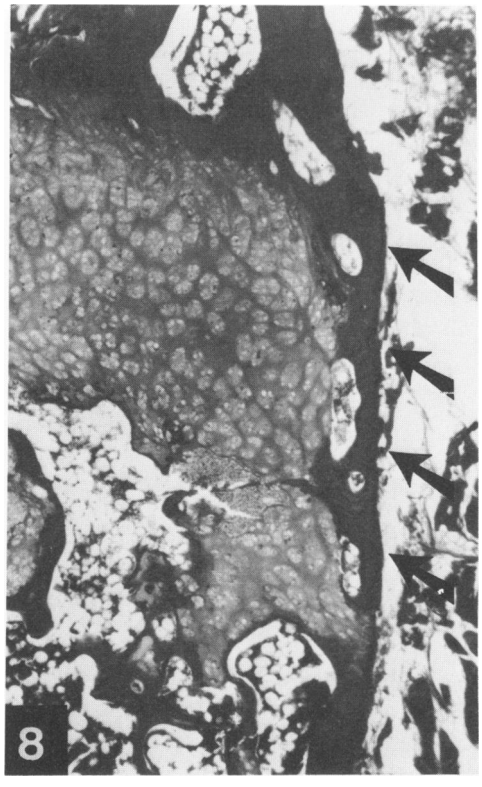
8

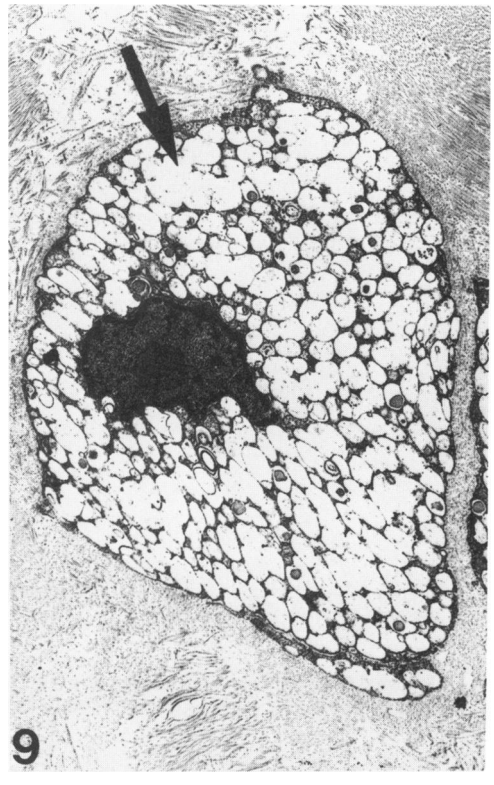
9

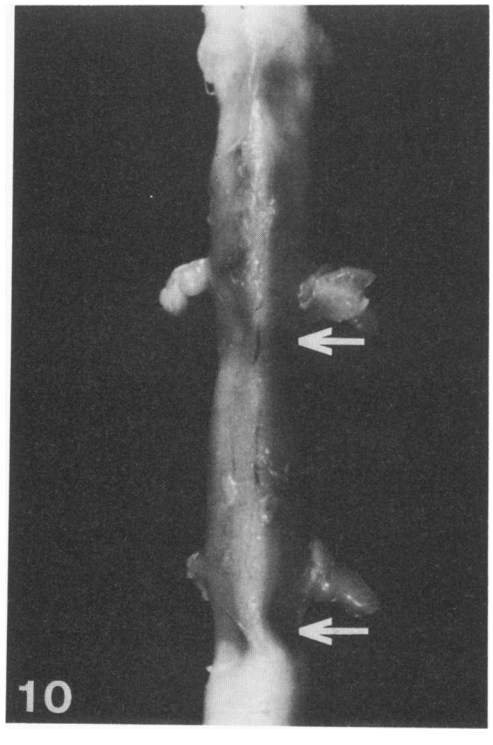
10


11

Figure 12—Light micrograph of the mitral valve. Note the large round cells with vesicular cytoplasm (*arrows*). (H&E, ×160)

Figure 13—Electron micrograph of a cell from the mitral valve, filled with membrane-bound empty inclusions. (Uranyl acetate–lead citrate, ×1900)

Figure 14—Light micrograph of the swollen smooth muscle cells of the aortic media. (Uranyl acetate-lead citrate, ×100)

Figure 15—Electron micrograph of a bone marrow granulocyte that contains numerous large membrane bound granular inclusions. (Uranyl acetate–lead citrate, ×4800)

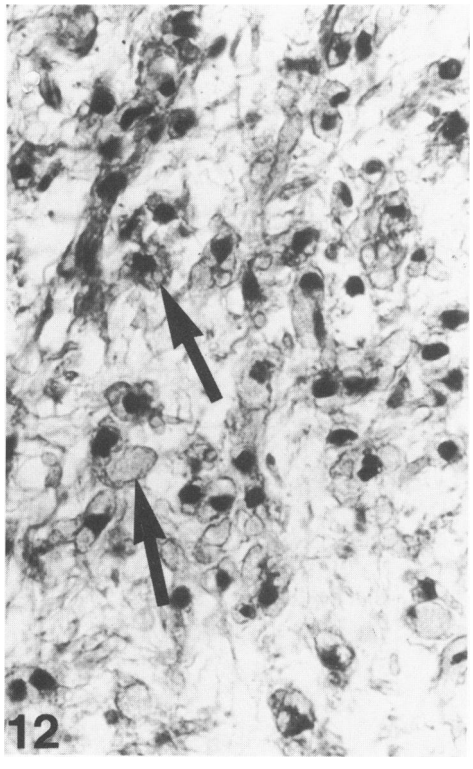
12

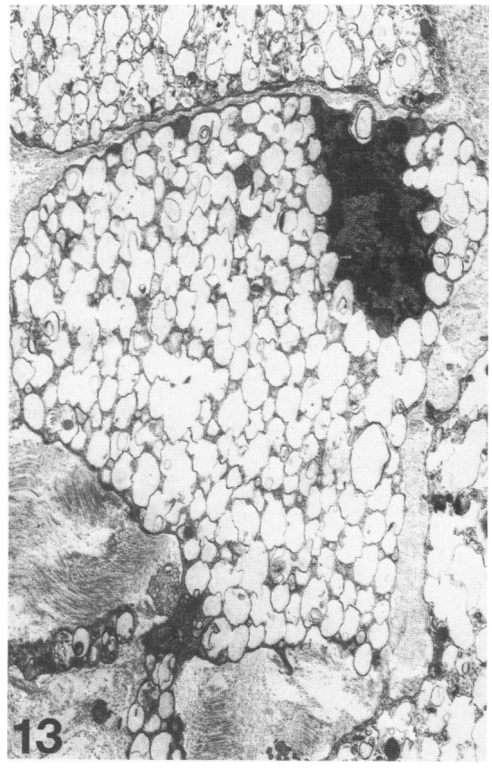
13

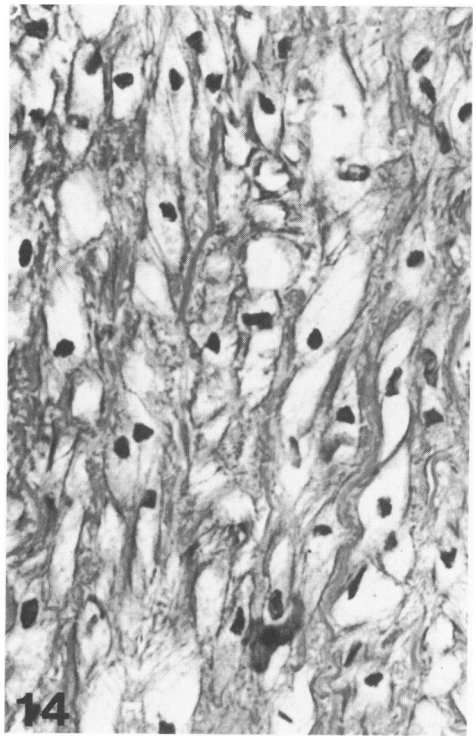
14

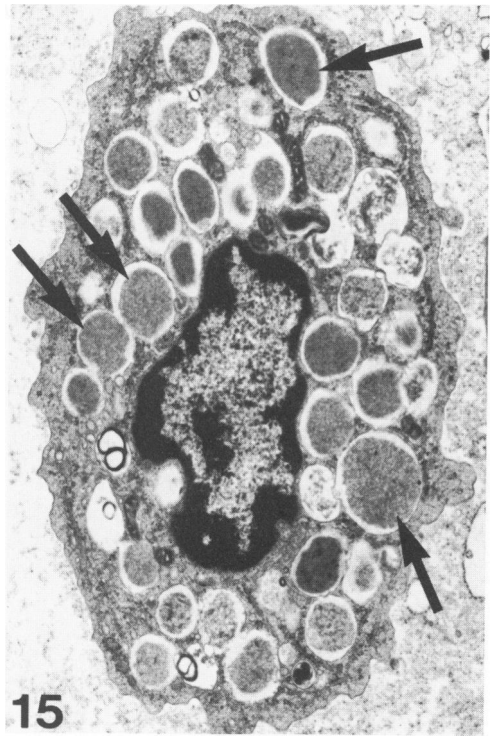
15

[*End of Article*]